TRANSLATION
2016, VOL. 4, NO. 1, e1138018 (12 pages)
http://dx.doi.org/10.1080/21690731.2015.1138018

Taylor & Francis
Taylor & Francis Group

PERSPECTIVE

Characterizing inactive ribosomes in translational profiling

Botao Liu[a,b,#] and Shu-Bing Qian[a,b]

[a]Division of Nutritional Sciences, Cornell University, Ithaca, NY, USA; [b]Graduate Field of Genetics, Genomics, and Development, Cornell University, Ithaca, NY, USA

ABSTRACT

The broad impact of translational regulation has emerged explosively in the last few years in part due to the technological advance in genome-wide interrogation of gene expression. During mRNA translation, the majority of actively translating ribosomes exist as polysomes in cells with multiple ribosomes loaded on a single transcript. The importance of the monosome, however, has been less appreciated in translational profiling analysis. Here we report that the monosome fraction isolated by sucrose sedimentation contains a large quantity of inactive ribosomes that do not engage on mRNAs to direct translation. We found that the elongation factor eEF2, but not eEF1A, stably resides in these non-translating ribosomes. This unique feature permits direct evaluation of ribosome status under various stress conditions and in the presence of translation inhibitors. Ribosome profiling reveals that the monosome has a similar but not identical pattern of ribosome footprints compared to the polysome. We show that the association of free ribosomal subunits minimally contributes to ribosome occupancy outside of the coding region. Our results not only offer a quantitative method to monitor ribosome availability, but also uncover additional layers of ribosome status needed to be considered in translational profiling analysis.

ARTICLE HISTORY
Received 28 October 2015
Revised 20 December 2015
Accepted 28 December 2015

KEYWORDS
elongation factors; profiling; ribosome; translation

Introduction

Translation can be divided mechanistically into 4 phases: initiation, elongation, termination and ribosome recycling.[1,2] Eukaryotic initiation begins with the recruitment of the small ribosomal subunit (40S) to the mRNA mainly via the recognition of 5′ cap structure. Following a scanning process, the selection of a start codon is accompanied with joining of the large ribosomal subunit 60S.[3,4] The formation of 80S ribosome at the start codon is followed by repetitive elongation steps mediated by elongation factors eEF1A and eEF2. eEF1A delivers aminoacylated tRNA to the ribosomal A site, whereas eEF2 catalyzes ribosomal translocation after formation of the peptide bond.[5] Once the 80S ribosome encounters a stop codon, termination occurs by the concerted action of release factors eRF1 and eRF3. Together with the ATP-binding cassette protein ABCE1, the terminating ribosome splits into free 60S and 40S subunits.[6] During ribosome recycling, a new round of translation is initiated by various factors on the released 40S subunits. Such a cyclical process is crucial in maintaining the overall translation efficiency by supplying the translation machinery in a continuous manner.

Given the tremendous energy cost associated with protein synthesis, it is not surprising that global protein synthesis is generally suppressed under a diverse array of stress conditions.[7,8] Indeed, many stress signaling pathways converge on key initiation factors, thereby limiting ribosome loading on mRNAs in response to stress.[9,10] It is anticipated that once the cap-dependent translation initiation is inhibited, the unused ribosomal subunits accumulate inside cells. Despite the fact that some ribosomes are utilized for cap-independent mRNA translation,[11] very little is known about the behavior of free ribosomes in surplus. Under certain types of stress, some 40S ribosomal subunits are re-located into stress granules, serving as a stress response pathway.[12] When the free ribosome subunits are not engaged with any messengers, one imminent question is whether they re-associate into empty 80S ribosomes, maintain separate subunits, or actively disassemble into ribosomal proteins.

CONTACT Shu-Bing Qian sq38@cornell.edu 301 Biotech, 526 Campus Road, Cornell University, Ithaca, NY 14853, USA.
[#]Present address: Program in Molecular Medicine, University of Massachusetts Medical School, Worcester, MA, USA.
Supplemental material data for this article can be accessed on the publisher's website.

Sucrose gradient-based polysome profiling has been commonly used to separate free ribosomal subunits, monosomes, and polysomes.[13] Given that actively translating mRNAs are often associated with multiple ribosomes, calculating the ratio of mRNA abundance in different fractions has been widely used as a measure of translational status under different growth conditions.[14] Consistent with this notion, many stress conditions lead to evident polysome disassembly with a corresponding increase of 80S monosome.[15] However, a substantial amount of ribosomes in the 80S fraction are empty as evidenced by the increased sensitivity to high salt treatment.[16] It is unclear whether these empty ribosomes are simple byproducts during sample preparation or bear unappreciated biological information. Recent development of ribosome profiling technology, based on deep sequencing of ribosome-protected mRNA fragments (RPFs), enables monitoring of ribosome position and density at the genome-wide scale.[17] However, ribosome profiling is not poised to capture empty ribosomes. Interestingly, ribosome profiling reveals pervasive footprints outside of protein-coding regions.[18] The central dilemma that confronts researchers concerns whether the ribosome occupancy at the non-coding region represents true translation events or simple artifacts arisen from rebinding of free ribosomal subunits. It is thus crucial to exclude false positive ribosome footprints in the profiling analysis.

Here we report that empty ribosomes present in cell lysates can be evaluated based on their stable association with the elongation factor eEF2. Direct comparison of ribosome footprints between monosome and polysome fractions reveals distinct pattern of ribosome dynamics. In addition, the free ribosomal subunits minimally contributes to ribosome occupancy at the non-coding region. Our results not only offer a simple method to monitor ribosome availability, but potentially uncover additional layers of ribosome status needed to be considered in many translational profiling analyses.

Results

Differential distribution of elongation factors between monosome and polysome

Sucrose gradient-based sedimentation has been widely used for separation of 40S, 60S, 80S, and polysomes from cell extracts. Although the 80S fraction contains empty ribosomes, the polysome is composed of actively translating ribosomes. eEF1A and eEF2 are mutually exclusive in binding to the ribosomal A-site and are expected to be present in the translating ribosomes.[1] To our surprise, in ribosome fractions obtained from HEK293 cells, both elongation factors were mainly located in the light fractions with few of these molecules detectable in the polysome fraction (Fig. 1A, left panel). A closer examination revealed that the 80S fraction contained more eEF2 than eEF1A, despite the fact that eEF1A is more abundant in cells.[19] This result is consistent with the previous study in *S. cerevisiae* using quantitative mass spectrometry, in which EFT2 (the yeast homolog of eEF2) and TEF2 (the yeast homolog of eEF1A) were primarily co-purified with the monosome rather than the polysome.[20] In addition, more EFT2 was present in the monosome fraction of yeast cells.[20]

It is possible that both elongation factors bind to the actively translating ribosomes with a fast kinetics and the association is not stable enough in the lysis buffer. To test this possibility, we conducted *in vivo* crosslinking before cell lysis using a Lomant's reagent DSP that is cleavable by reducing agent. Despite the improved recovery of eEF1A and eEF2 in the polysome fraction, both elongation factors were still highly concentrated in the light fractions (Fig. S1). In particular, the dominant presence of eEF2 in the monosome suggests that the ribosome in this fraction differs from the one undergoing active translation.

Prominent eEF2 association with ribosomes under proteotoxic stress

We next attempted to increase the monosome fraction of HEK293 cells by applying proteotoxic stress that potently attenuates global protein synthesis.[15] Pre-exposure of cells to a proline analog $_{L}$-azetidine-2-carboxylic acid (AZC) and a proteasome inhibitor MG132 markedly reduced the polysome with a pronounced increase in the monosome (Fig. 1A, right panel). Interestingly, only eEF2, but not eEF1A, showed a corresponding increase in the monosome. This pattern was maintained after in vivo crosslinking using DSP (Fig. S1). To examine the ribosome-associated elongation factors in a more quantitative manner, we spin down all the ribosomes through a sucrose

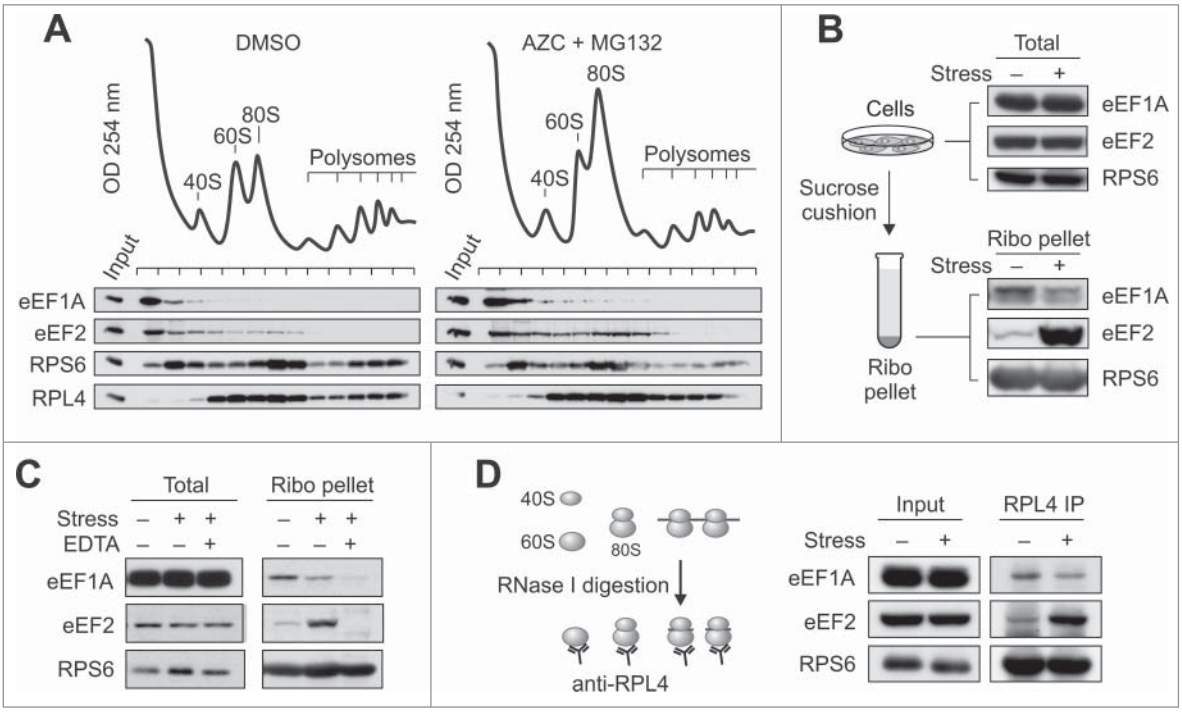

Figure 1. Differential association of elongation factors with ribosomes (A) HEK293 cells were pre-treated with 10 mM AZC and 20 μM MG132 (right panel) or DMSO control (left panel) for 60 min followed by sucrose gradient sedimentation. Both the whole cell lysates (input) and ribosomes fractions were immunoblotted using antibodies indicated. (B) Sucrose cushion analysis of ribosome-associated elongation factors in HEK293 cells with or without proteotoxic stress. Both the whole cell lysates (total) and ribosome pellets were immunoblotted using antibodies indicated. (C) Sucrose cushion analysis of ribosome-associated elongation factors in samples as (B) in the presence of absence of 40 μM EDTA. (D) Ribosome immunoprecipitation analysis of ribosome-associated elongation factors. Whole cell lysates as (B) were treated with RNase I to convert polysome into monosome followed by anti-RPL4 immunoprecipiatation.

cushion (Fig. 1B). For cells under proteotoxic stress, eEF1A showed a minor but obvious reduction in the ribosome pellet. Remarkably, eEF2 exhibited a striking accumulation in the same ribosome pellet. The eEF2 co-sedimentation is a result of association with the 80S ribosome because EDTA treatment greatly abolished the accumulation of both elongation factors (Fig. 1C). To exclude the non-specific eEF2 association in the ribosome pellet, we purified ribosomes using affinity immunoprecipitation (IP) from cell lysates treated with RNase I to convert all ribosomes into monosome (Fig. 1D). Consistent with the sucrose cushion result, less eEF1A but more eEF2 molecules were precipitated from stressed cells by an antibody against RPL4, a core ribosomal protein. This result suggests that eEF2 preferentially associates with non-translating ribosomes.

eEF2 preferentially associates with empty ribosomes

We previously demonstrated that proteotoxic stress caused an early ribosomal pausing on mRNAs.[15] It is unclear whether eEF2 preferentially binds to the paused ribosome or the empty ribosome without mRNA. To distinguish these 2 possibilities, we conducted nascent chain IP to collect specific mRNA-engaged ribosomes followed by detection of elongation factors (Fig. S2). Consistent with the early pausing,[15] more ribosomes were associated with the nascent chain in the presence of AZC and MG132. However, proteotoxic stress did not lead to any accumulation of eEF2 in the purified ribosomes synthesising Flag-GFP. This result further suggests that eEF2 preferentially associates with empty ribosomes without mRNA engagement.

Many stress conditions lead to an increased monosome fraction as a result of repression in global protein synthesis.[21] If eEF2 preferentially binds to empty ribosomes, then different types of stress would lead to the same consequence. Indeed, oxidative stress by sodium arsenite treatment or heat shock stress potently induced eEF2 accumulation in the ribosome pellet (Fig. 2A). In contrast, eEF1A showed a corresponding decrease in the

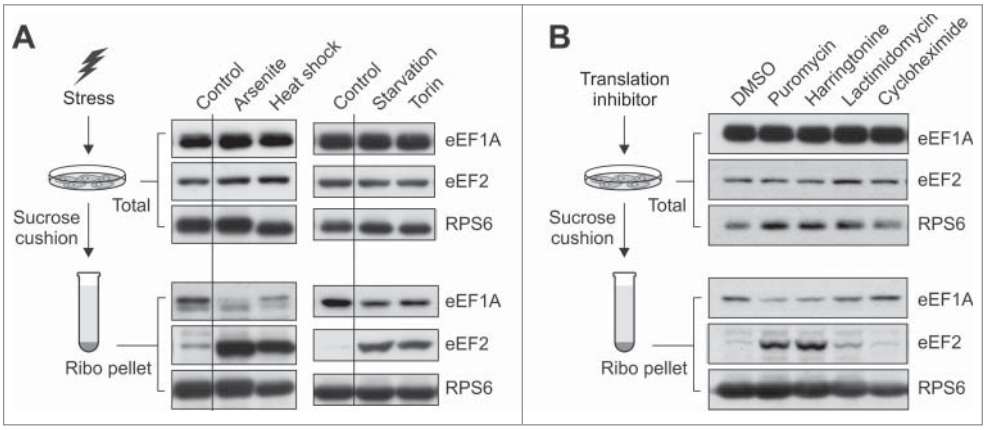

Figure 2. eEF2 stably associates with empty ribosomes. (A) Sucrose cushion analysis of ribosome-associated elongation factors in HEK293 cells under various stress conditions, including arsenite (0.5 mM for 60 min), heat shock (43°C for 60 min), amino acid starvation (60 min), or torin (250 nM for 60 min). Both the whole cell lysates (total) and ribosome pellets were immunoblotted using antibodies indicated. Black line indicates that some intervening lanes were removed from the same gel image. (B) Sucrose cushion analysis of ribosome-associated elongation factors in HEK293 cells under various tress conditions, including puromycin (100 μM for 60 min), harringtonine (2 μg/mL for 60 min), lactimidomycin (50 μM for 60 min), or cycloheximide (100 μM for 60 min). Both the whole cell lysates (total) and ribosome pellets were immunoblotted using antibodies indicated.

same samples. To substantiate the finding further, we suppressed cap-dependent translation initiation by applying amino acid starvation or treating cells with Torin, a potent inhibitor of mammalian target of rapamycin complex I (mTORC1).[22] Both conditions unequivocally led to eEF2 build-up in the ribosome pellet with a corresponding decrease of eEF1A (Fig. 2A).

To definitively demonstrate that eEF2 associates with empty ribosomes only, we took advantage of a panel of translation inhibitors. Puromycin acts as a tRNA analog, releases the nascent chain from the ribosome P-site, and dissociates the ribosome into separate subunits.[23] As expected, puromycin treatment completely disassembled the polysome with a dramatic increase of the monosome fraction (Fig. S3). Similar to many stress conditions aforementioned, puromycin treatment resulted in a prominent accumulation of eEF2 in the ribosome pellet (Fig. 2B). The elongation inhibitor cycloheximide is known to stabilize the polysome by immobilizing ribosomes on the mRNA, thereby limiting the amount of free ribosomes. As a result, few eEF2 was detectable in the ribosome pellet from cells after cycloheximide treatment. Notably, the inverse correlation between eEF2 and eEF1A was evident in these ribosome pellets. Thus, the relative ratio of these 2 elongation factors can be used to evaluate the ribosome status in a quantitative manner.

We next tested 2 additional translation inhibitors known to immobilize the initiating ribosome. Harringtonine binds to the free 60S ribosome subunit and prevents the first peptide bond formation upon the 80S assembly.[24] Despite the potential enrichment of ribosomes at the initiation sites,[25] a substantial amount of eEF2 was accumulated in the ribosome pellet (Fig. 2B). This result suggests that a large portion of ribosomes cannot undergo initiation in the presence of harringtonine. Alternatively, the harringtonine-immobilized ribosomes are not stable. Unlike harringtonine, lactimidomycin preferentially acts on the initiating ribosomes by binding to the empty E-site.[26] In cells treated with lactimidomycin, fewer eEF2 molecules were recovered from the ribosome pellet in comparison to harringtonine treatment (Fig. 2B). Although lactimidomycin permits new rounds of initiation that uses free ribosomes, [27] we cannot exclude the possibility that the presence of this compound may prevent stable eEF2 binding to the empty ribosome.

Examining empty ribosomes by ribosome profiling

Given the increasing popularity of ribosome profiling in studying translational regulation,[28] we wonder whether the presence of empty ribosomes might perturb high-throughput sequencing of ribosome footprints. We reason that the empty 80S ribosomes are likely formed by simple re-association of free 40S

and 60S subunits in the lysis buffer. The lack of mRNA permits stable eEF2 binding. However, such random association of ribosomal subunits could lead to promiscuous binding to various RNA species present in the lysates. These non-translating ribosomes could leave non-specific footprints that are indistinguishable from true footprints. These false positives, if present, are likely to be amplified under stress conditions because of the large amount of free ribosomes after severe translational inhibition.

Since the majority of empty ribosomes co-migrate with the 80S monosome on the sucrose gradient, we separated the 80S monosome from the total fractions using HEK293 lysates (Fig. 3A). Both samples were then subject to RNase I digestion followed by library construction. We omitted the rRNA-depletion step so we could count total reads mapped to mRNA and rRNA respectively. Empty ribosomes are expected to give rise to reads derived from rRNA only, but not mRNA. Indeed, the monosome showed a 4-fold lower mRNA/rRNA ratio in comparison to the total fractions (Fig. 3B and Table 1). It is possible that the increased rRNA reads in the monosome were partially derived from the contaminated free 40S and 60S subunits. By taking into account their maximal OD254 value, still approximately half of the monosomes are not associated with any mRNA fragments. Despite the increased proportion of rRNA reads in the monosome fraction, individual rRNA read maps were comparable between the 2 samples (Fig. S4). The highly clustered rRNA read pattern is consistent with the structure of mammalian ribosomes with many rRNA segments exposed outside.[29] The similar rRNA read pattern in all the ribosome fractions suggests that the empty 80S

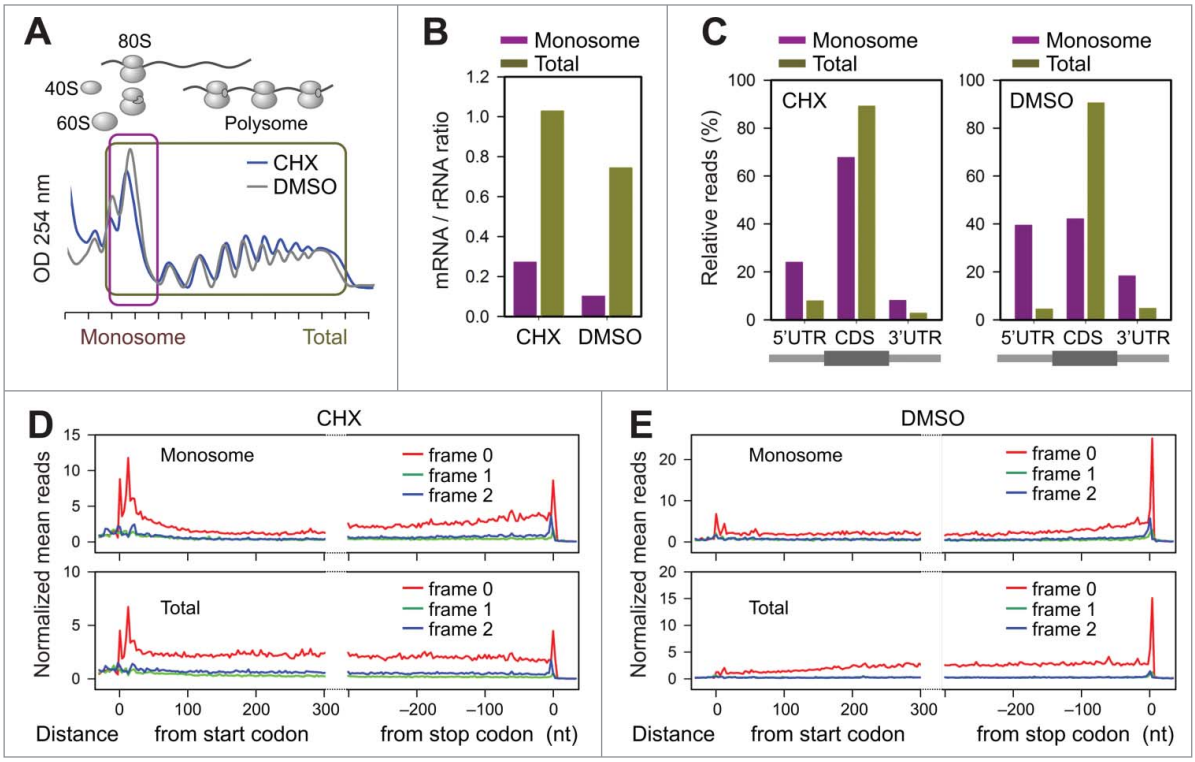

Figure 3. Examine empty ribosomes by ribosome profiling. (A) Sucrose gradient sedimentation of whole cell lysates from HEK293 cells in the absence (DMSO, gray line) or presence of 100 μM cycloheximide (CHX, blue line). Both the monosome (purple box) and the total fraction (dark yellow box) were collected for ribosome profiling. (B) The monosome and total ribosomes fractions shown in (A) were subject to separate ribosome profiling. Relative ratio of reads mapped to mRNA and rRNA was used to evaluate the amount of empty ribosomes in the monosome. (C) Fractions of reads mapped to different regions of mRNA were quantified for the monosome (left panel) and the total fractions (right panel) as shown in (A). (D) Metagene analysis of ribosome-protected fragments derived from the monosome (top panel) or the total fraction (bottom panel) in the presence of 100 μM cycloheximide. Normalized reads are averaged across the transcriptome, aligned at either their start or stop codons. Different reading frames are color coded. (**E**) Metagene analysis of ribosome-protected fragments derived from the monosome (top panel) or the total fraction (bottom panel) in the absence of 100 μM cycloheximide.

ribosome resembles the translating ribosomes in terms of the overall conformation.

Interpreting monosome in the presence of empty ribosomes

With the presence of large quantity of empty ribosomes, the increased rRNA reads would reduce the mRNA read depth in the monosome. However, we are more concerned whether some of these inert ribosomes would randomly bind to mRNA species. This concern arises from traditional *in vitro* translation experiments, in which purified ribosome subunits readily bind to the poly(U) template independent of initiation factors.[30] If random binding occurs in the current system, the resultant false footprints would increase the read density in the non-coding region and decrease the 3-nt periodicity (phasing) in the coding region. Compared to the reads obtained from total fractions, monosome-derived footprints showed higher occupancy in the non-coding region, in particular 5′UTR (Fig. 3C). However, the 5′UTR ribosome occupancy could result from uORF translation, which is over-represented in the monosome because of the linear scanning process of initiating ribosomes.[31] Notably, both the monosome and the total fractions maintained a dominant single reading frame (Fig. S5A), arguing against the random association of free ribosomal subunits on transcripts.

Interestingly, the monosome demonstrated a distinct pattern of read distribution in comparison to the total fractions. Unlike the polysome that exhibits uniform distribution of reads along the CDS, the monosome showed fewer reads in the middle region of the CDS (Fig. 3D). This result is consistent with the notion that ribosome moves relatively slower shortly after initiation and before termination.[32] In polysomes, however, prolonged pausing of the leading ribosome often leads to stacking of the following ribosomes, causing increased ribosome density at multiple positions. Without the influence of neighboring ribosomes, the monosome fraction may be more valuable than the polysome in revealing elongation speed and assessing decoding kinetics.[33,34]

To further exclude the possibility of non-specific ribosome binding, we sought to increase the amount of free ribosomal subunits in cells. Many stress conditions lead to increased free ribosomes as a result of translation inhibition (Fig. 2A). However, non-canonical translation could also be induced under these conditions and it is difficult to distinguish true uORF translation from non-specific footprints. We therefore chose to increase the amount of free ribosomes without changing the growth condition. Ribosome profiling typically uses translation inhibitors like cycloheximide to immobilize ribosomes on transcripts.[35] In the absence of translation inhibitors, some ribosomes are expected to run off. Indeed, without cycloheximide treatment, the polysome was slightly reduced with a concomitant increase of monosome (Fig. 3A). Consistent with the runoff process, a substantial amount of reads were migrated toward the end of the CDS, including the stop codon (Fig. 3E). Further supporting the formation of more empty ribosomes in the absence of cycloheximide, a lower mRNA/rRNA read ratio was evident in all ribosome fractions (Fig. 3B).

Among the reads mapped to transcriptome in the absence of cycloheximide, the monosome showed a drastic reduction of CDS occupancy relative to the cycloheximide-treated sample (Fig. 3C, right panel). Despite the lower ribosome density in the absence of cycloheximide, the monosome maintained the strong 3-nt periodicity in the CDS region (Fig. S5B). Therefore, free ribosomal subunits do not undergo non-specific mRNA binding, at least to the coding region. Notably, the apparent increase of read density in both 5′UTR and 3′UTR regions is not an absolute value. When the total read amount is normalized for the monosome, the amount of 3′UTR read density was maintained at the similar levels in the presence or absence of cycloheximide (Fig. S6A). This is consistent with the notion that the 3′UTR occupancy likely represents background signals, presumably due to the presence of RNA-binding protein (RNPs) co-migrating with ribosomes [18]. Supporting this notion, reads mapped to 3′UTR showed neither dominant reading frames nor typical read length distribution (Fig. S6B and C). Since no additional reads were detected above the background signals of 3′UTR, the increased free ribosomes in the absence of cycloheximide does not contribute to ribosome occupancy outside of the coding region.

Discussion

It has been estimated that a typical mammalian cell contains about 3,000,000 ribosomes. However, the

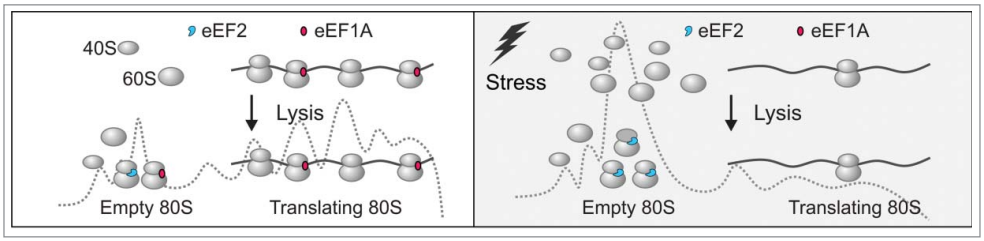

Figure 4. Multiple ribosome status in translational profiling. A schematic model depicting different ribosome status in cells. Under the normal growth condition (left panel), multiple ribosomes are loaded onto single transcripts, leaving fewer ribosomal subunits and empty ribosomes. Under stress conditions (right panel), global repression of translation leads to accumulation of free ribosomal subunits that tend to form empty ribosomes stably associated with eEF2.

quantity of total mRNAs is less than 300,000 per cell.[36] Although polysomes are common in proliferating cells, not all the transcripts are equally used for active translation.[37] It is therefore not surprising to find many empty ribosomes in cells even under the normal growth condition. Upon stress, global translation repression leads to more free ribosomes that potentially influence the intracellular milieu. However, the presence of large quantity of non-translating ribosomes is virtually ignored in most translational profiling analysis. The ability to quantify empty ribosomes at any given cellular stage will aid in our understanding of translational regulation.

Despite long appreciation of the spare ribosomes in cells, no simple way is available to distinguish empty ribosomes from translating ribosomes. A commonly used approach relies on high salt sensitivity of the 80S ribosome fraction separated on a sucrose gradient.[16] Although informative, the salt sensitivity can be influenced by many confounding factors in the buffer system and does not offer reliable quantification. We found that empty ribosomes preferentially bind to eEF2, an elongation factor that is essential for translocation. Surprisingly, eEF2 is largely absent in polysomes captured by sucrose gradient sedimentation, which is consistent with the transient nature of the translocation process (within milliseconds).[38] In prokaryotes, EF-G can be trapped on the translating ribosome only by using nonhydrolyzable analogs of GTP as demonstrated in recent crystal structures of 70S ribosomes.[39-41] Interestingly, mammalian ribosomes prepared using high salt led to constant presence of eEF2, but not other translation factors.[29,42,43] Our results clearly indicate that eEF2 stably binds to empty ribosomes, although we do not know whether the binding occurs inside cells or in the lysis buffer. Regardless, it is clear that the level of ribosome-bound eEF2 is proportional to the amount of free ribosomes. This feature offers a sensitive means to evaluate ribosome availability under various stress conditions (Fig. 4). In addition, it provides unique aspects of ribosome status in the presence of different translation inhibitors.

Classic translation assays using a reconstituted *in vitro* system demonstrated that purified ribosomal subunits can associate with poly(U) to direct the synthesis of polyphenylalanine in the absence of initiation factors.[44] The large quantity of mRNA-free ribosomes present in the monosome raises an imminent question about the possibility of random ribosome binding to transcripts. This issue is particularly important in deep sequencing-based ribosome profiling.[28] Indeed, this approach reveals pervasive ribosome occupancy outside of annotated protein-coding regions, including 5′UTRs as well as long intergenic noncoding RNAs (lincRNAs).[18] Although mass spectrometry experiments confirmed the existence of some peptides derived from these non-coding regions,[45,46] the question lingers whether all of these ribosomes are truly undergoing active translation. A growing body of evidence suggests that ribosome engagement has impacts beyond the production of polypeptides. However, it is crucial to exclude false positive ribosome footprints in the profiling analysis. Those non-specific ribosome binding include, but not limited to, random association of free ribosomal subunits and constant binding of RNPs co-sedimented with ribosome. We provide experimental evidence that free subunits undergo minimal non-specific association on transcripts. This result is consistent with the recent report that mixing mammalian and yeast

cell lysates did not generate "cross-over" footprints, although the amount of free ribosomes was unclear.[18]

The significance of understanding different ribosome status is also reflected in recently established initiating ribosome profiling,[27] which has proven to be powerful in uncovering hidden coding potential of transcriptomes. These approaches often rely on elongating ribosome runoff that generates an enormous amount of free ribosomes highly enriched in the monosome.[25,27,47,48] Given the unique feature of eEF2 binding, we anticipate that it is now possible to deplete empty ribosomes from the monosome by using anti-eEF2 antibodies. We are currently testing this possibility as part of the continuous optimization of existing profiling protocols. Taken together, our results provide a useful platform for further improvement of translational profiling, experimentally and analytically.

Materials and methods

Cells and reagents

HEK293 cells were maintained in Dulbecco's Modified Eagle's Medium (DMEM) with 10% fetal bovine serum (FBS). $_{L}$-azetidine-2-carboxylic acid (AZC), Z-Leu-Leu-Leu-al (MG132), sodium arsenite ($NaAsO_2$), cycloheximide (CHX), Ethylenediaminetetraacetic acid (EDTA), puromycin and secondary antibodies were purchased from Sigma. Torin (Tocris bioscience) and harringtonine (LKT Laboratories) were also purchased. Lactimidomycin was generously provided by Dr. Ben Shen (Scripps, Florida). Anti-rpS6 (Cell signaling), anti-eEF2 (Cell signaling), anti-eEF1A (Millipore), and anti-rpL4 (ProteinTech) antibodies were acquired. Dithiobis[succinimidyl propionate]; (DSP) and sucrose were from Thermo Fisher Scientific.

Ribosome separation on sucrose gradient

Polysome buffer (pH 7.4, 10 mM HEPES, 100 mM KCl, 5 mM $MgCl_2$) was used to prepare all sucrose solutions. Sucrose density gradients (15%–45% w/v) were freshly made in SW41 ultracentrifuge tubes (Backman) using a Gradient Master (BioComp Instruments) according to manufacturer's instructions. Cells were pre-treated with 100 μg/ml cycloheximide for 3 min at 37°C to stabilize ribosomes on mRNAs followed by washing using ice-cold PBS containing 100 μg/ml cycloheximide. Cells were then lysed on ice by scraping extensively in polysome lysis buffer (pH 7.4, 10 mM HEPES, 100 mM KCl, 5 mM $MgCl_2$, 100 μg/ml cycloheximide and 2% Triton X-100). Cell debris were removed by centrifugation at14,000 rpm for 10 min at 4°C. 600 μl of supernatant was loaded onto sucrose gradients followed by centrifugation for 150 min at 32,000 rpm 4°C in a SW41 rotor. Separated samples were fractionated at 1.5 ml / min through a fractionation system (Isco) that continually monitored OD_{254} values. Fractions were collected with 0.5 min interval. For DMSO samples, CHX in all buffers was replaced with equal amount of DMSO. For puromycin treatment, 100 μM puromycin was added during the pre-treatment instead of CHX.

For the DSP crosslinking, medium was aspirated out and cells were washed once with PBS (RT) to remove free amino acid residuals as much as possible. Crosslinking was performed with 2.5 mM DSP in PBS (RT) at RT for 1 min and quenched with 50 mM Tris (pH7.0) at RT for 1 min. After the aspiration of supernatants, cells were washed with ice-cold PBS (100 μg/ml CHX) once and lysed with polysome lysis buffer. Before immunoblotting, crosslinking was reversed by incubating samples in sample buffer (with100 mM DTT) at 37°C for 30 min.

Ribosome pelleting on sucrose cushion

300 μl cleared lysate was laid on top of 900 μl 1M sucrose in Beckman centrifugation tubes. Ribosomes were pelleted by centrifugation at 78,000 rpm for 120 min at 4°C using a Beckman TLA-110 rotor. After removing the supernatant, ribosome pellets were rinsed with polysome buffer once and resuspended in sample buffer (50 mM Tris-HCl, pH 6.8, 100 mM dithiothreitol, 2% SDS, 0.1% bromophenol blue, 10% glycerol) for immunoblotting.

Immunoprecipitation and immunoblotting

Cells were pre-treated with 100 μg/ml cycloheximide at 37°C for 3 mins to stabilize ribosome complexes and washed once with ice-cold PBS plus 100 μg/ml CHX. Cells were then scraped extensively in polysome lysis buffer supplemented with EDTA-free cocktail protease inhibitor (Roche). After clearance by centrifugation for 10 min at14,000 rpm at 4°C, the supernatant was collected and incubated with 200 U RNaseI (Ambion) and anti-RpL4 antibody at 4°C for 1 h. After that, protein A beads previously equilibrated

with polysome lysis buffer were incubated with the mixture at 4°C for 1 h. Beads were washed for 3 times with polysome lysis buffer and associated proteins were eluted by heating at 95°C for 10 min in the sample buffer. For immunoprecipitation of ribosome-associated nascent chains, lysate was incubated with anti-Flag M2 affinity gel (Sigma) at 4°C for 1 h without RNaseI digestion.

For immunoblotting, protein samples were resolved on SDS-PAGE and then transferred to Immobilon-P membranes (Millipore). After blocking for 1 hour in TBS containing 5% blotting milk, membranes were incubated with primary antibodies at 4°C overnight. After incubation with horseradish peroxidase–coupled secondary antibodies, immunoblots were developed using enhanced chemiluminescence (GE Healthcare). Densitometry is used to quantify the immunoblotting bands. In brief, specific bands with equal surface areas were selected using ImageQuant followed by gray scale measurement. A blank areas was also include as background levels. Relative ratio was calculated using control as 1.

Ribosome profiling

Sucrose gradient fractions corresponding to only monosome or monosome with polysome were pooled and a 200 μl aliquot was digested with 200U *E. coli* RNase I (Ambion) at 4°C for 1 h. Total RNAs were extracted using Trizol reagent (Invitrogen). Subsequently, RNA molecules were dephosphorylated by 20U T4 polynucleotide kinase (NEB) in the presence of 10 U SUPERase (Ambion) at 37°C for 1 hour. The enzyme was heat-inactivated for 20 min at 65°C. The products were then separated on a Novex denaturing 15% polyacrylamide TBE-urea gel (Invitrogen). Gel bands corresponding to 28-30 nt RNA molecules were excised and physically disrupted by centrifugation through the holes of the tube. Resulting gel debris was soaked overnight in the RNA gel elution buffer (300 mM NaOAc pH 5.5, 1 mM EDTA, 0.1 U/μl SUPERase_In) to recover RNA fragments. The gel debris was filtered out with a Spin-X column (Corning) and RNA was finally purified using ethanol precipitation.

The cDNA library construction was described [27]. In brief, Poly-A tails were added to the purified RNA fragments by E. coli poly-(A) polymerase (NEB) with 1 mM ATP in the presence of 0.75 U/μL SUPERase_In at 37°C for 45 min. The tailed RNA molecules were reverse transcribed to generate the first strand cDNA using SuperScript III (Invitrogen) and following oligos containing barcodes:

MCA02, 5′-pCAGATCGTCGGACTGTAGAACTCT Ø CAAGCAGAAGACGGCATACGATT TTTTTTTTT TTTTTTTTTVN-3′;

LGT03, 5′-pGTGATCGTCGGACTGTAGAACTCT Ø CAAGCAGAAGACGGCATACGATT T TTTTTTTTTTTTTTTTTVN-3′;

YAG04, 5′-pAGGATCGTCGGACTGTAGAACTCT Ø CAAGCAGAAGACGGCATACGATT TTTTTTTTTTT TTTTTTTVN-3′;

HTC05, 5′-pTCGATCGTCGGACTGTAGAACTC T Ø CAAGCAGAAGACGGCATACGATT TTTTTTTTTTTTTTTTTVN-3′

Reverse transcription products were resolved on a 10% polyacrylamide TBE-urea gel as described above. The expected 92 nt band of first strand cDNA was excised and recovered as above using DNA gel elution buffer (300 mM NaCl, 1 mM EDTA). Purified first strand cDNA was then circularized by 100U CircLigase II (Epicentre) following manufacturer's instructions. The resulting circular single strand DNA was purified using ethanol precipitation and re-linearized by 7.5 U APE 1 in 1 X buffer 4 (NEB) at 37°C for 1 h. The products were resolved on a Novex 10% polyacrylamide TBE-urea gel (Invitrogen) as described above. The expected 92 nt band was then excised and recovered. Finally, single-stranded template was amplified by PCR using the Phusion High-Fidelity enzyme (NEB) according to the manufacturer's instructions. The primers qNTI200 (5′-CAAGCAGAAGACGGCATA-3′) and qNTI201 (5′-AATGATACGGCGACCACCG ACAGGTTCAGAGTTCTACAGTCCGACG-3′) were used to create DNA library suitable for sequencing. The PCR reaction contains 1× HF buffer, 0.2 mM dNTP, 0.5 μM primers, 0.5U Phusion polymerase. PCR was carried out with an initial 30 s denaturation at 98°C, followed by 12 cycles of 10 s denaturation at 98°C, 20 s annealing at 60°C, and 10 s extension at 72°C. PCR products were separated on a non-denaturing 8% polyacrylamide TBE gel as described above. Expected 120 bp band was excised and recovered as described above. After quantification by Agilent BioAnalyzer DNA 1000 assay, equal amount of barcoded samples were pooled into one sample. 3 ~ 5 pmol mixed DNA samples were

Table 1. Statistics of ribosome profiling.

Sample	Total	Trimmed 25-35	Mapped to rRNA	Mapped to mRNA
DMSO_Mono	21492787	15589353	6895309	698,779
CHX_Mono	22612056	17822729	7635030	2,071,271
DMSO_Total	22733871	11162662	4659077	3,461,257
CHX_Total	23620446	17601268	6534415	6,719,868

typically used for cluster generation followed by sequencing using sequencing primer 5′-CGA-CAGGTTCAGAGTTC TACAGTCCGACGATC-3′ (HiSEQ2000, Cornell University Life Sciences Core Laboratories Center).

Data analysis

The next-generation sequencing data of ribosome footprints was processed and analyzed using a collection of custom Perl scripts. The barcoded multiplex sequencing output files were separated into individual sample datasets according to the first 2-nucleotide barcodes. To remove adaptor sequences, 7 nucleotides were cut from the 3′ end of each 50-nt-long Illumina sequence read, and the 3′ polyA tails were identified and removed allowing 1 mismatch. The high quality reads of length ranging from 25 to 35 nt were then retained while other reads were excluded from the downstream analysis. A set of longest mRNA transcripts and associated CDS annotation were compiled from RefSeq Human transcriptome reference (downloaded from NCBI on 09-17-2012) by comparing different mRNA isoforms of the same gene on CDS length (if CDS lengths are the same, 5′ UTR lengths are compared). The trimmed reads were first aligned to human rRNA sequences and unmapped reads were mapped to the representative longest mRNAs by Bowtie-0.12.3. One mismatch was allowed in all mappings; in cases of multiple mapping, mismatched positions were not used if a perfect match existed. Reads mapped more than 100 times were discarded to remove poly-A–derived reads. Finally, reads were counted at every position of individual transcripts by using the 13th nucleotide of the read for the P-site position. For the read aggregation plot, only mRNAs with at least 30nt UTR, 300nt CDS, and 50 mapped reads in all samples were included. The number of reads aligned to each position of individual mRNA was first normalized by the total number of reads recovered from the same mRNA. The read counts were then averaged across all mRNAs for each position relative to the annotated start or stop codon.

Disclosure of potential conflicts of interest

No potential conflicts of interest were disclosed.

Acknowledgements

We'd like to thank Qian lab members for helpful discussion. We also thank Cornell University Life Sciences Core Laboratory Center for performing deep sequencing.

Funding

This work was supported by grants to S.-B.Q. from US National Institutes of Health (R01AG042400), and US Department of Defense (W81XWH-14-1-0068).

References

[1] Jackson RJ, Hellen CU, Pestova TV. The mechanism of eukaryotic translation initiation and principles of its regulation. Nat Rev Mol Cell Biol 2010; 11:113-27; PMID:20094052; http://dx.doi.org/10.1038/nrm2838

[2] Sonenberg N, Hinnebusch AG. New modes of translational control in development, behavior, and disease. Mol Cell 2007; 28:721-9; PMID:18082597; http://dx.doi.org/10.1016/j.molcel.2007.11.018

[3] Aitken CE, Lorsch JR. A mechanistic overview of translation initiation in eukaryotes. Nat Struct Mol Biol 2012; 19:568-76; PMID:22664984; http://dx.doi.org/10.1038/nsmb.2303

[4] Hinnebusch AG. The scanning mechanism of eukaryotic translation initiation. Annu Rev Biochem 2014; 83:779-812; PMID:24499181; http://dx.doi.org/10.1146/annurev-biochem-060713-035802

[5] Kong J, Lasko P. Translational control in cellular and developmental processes. Nat Rev Genet 2012; 13:383-94; PMID:22568971; http://dx.doi.org/10.1038/nrg3184

[6] Jackson RJ, Hellen CU, Pestova TV. Termination and post-termination events in eukaryotic translation. Adv Protein Chem Struct Biol 2012; 86:45-93; PMID:22243581; http://dx.doi.org/10.1016/B978-0-12-386497-0.00002-5

[7] Holcik M, Sonenberg N. Translational control in stress and apoptosis. Nat Rev Mol Cell Biol 2005; 6:318-27; PMID:15803138; http://dx.doi.org/10.1038/nrm1618

[8] Liu B, Qian SB. Translational reprogramming in cellular stress response. Wiley Interdiscip Rev RNA 2014; 5 (3):301-15; PMID: 24375939; http://dx.doi.org/10.1002/wrna.1212

[9] Ma XM, Blenis J. Molecular mechanisms of mTOR-mediated translational control. Nat Rev Mol Cell Biol 2009; 10:307-18; PMID:19339977; http://dx.doi.org/10.1038/nrm2672

[10] Harding HP, Calfon M, Urano F, Novoa I, Ron D. Transcriptional and translational control in the Mammalian unfolded protein response. Annu Rev Cell Dev Biol 2002; 18:575-99; PMID:12142265; http://dx.doi.org/10.1146/annurev.cellbio.18.011402.160624

[11] Hellen CU, Sarnow P. Internal ribosome entry sites in eukaryotic mRNA molecules. Genes Dev 2001; 15:1593-612; PMID:11445534; http://dx.doi.org/10.1101/gad.891101

[12] Buchan JR, Parker R. Eukaryotic stress granules: the ins and outs of translation. Mol Cell 2009; 36:932-41; PMID:20064460; http://dx.doi.org/10.1016/j.molcel.2009.11.020

[13] Masek T, Valasek L, Pospisek M. Polysome analysis and RNA purification from sucrose gradients. Methods Mol Biol 2011; 703:293-309; PMID:21125498; http://dx.doi.org/10.1007/978-1-59745-248-9_20

[14] Arava Y, Wang Y, Storey JD, Liu CL, Brown PO, Herschlag D. Genome-wide analysis of mRNA translation profiles in Saccharomyces cerevisiae. Proc Natl Acad Sci U S A 2003; 100:3889-94; PMID:12660367; http://dx.doi.org/10.1073/pnas.0635171100

[15] Liu B, Han Y, Qian SB. Cotranslational response to proteotoxic stress by elongation pausing of ribosomes. Mol Cell 2013; 49:453-63; PMID:23290916; http://dx.doi.org/10.1016/j.molcel.2012.12.001

[16] Martin TE, Hartwell LH. Resistance of active yeast ribosomes to dissociation by KCl. J Biol Chem 1970; 245:1504-6; PMID:5442831

[17] Ingolia NT, Ghaemmaghami S, Newman JR, Weissman JS. Genome-wide analysis in vivo of translation with nucleotide resolution using ribosome profiling. Science 2009; 324:218-23; PMID:19213877; http://dx.doi.org/10.1126/science.1168978

[18] Ingolia NT, Brar GA, Stern-Ginossar N, Harris MS, Talhouarne GJ, Jackson SE, Wills MR, Weissman JS. Ribosome profiling reveals pervasive translation outside of annotated protein-coding genes. Cell Rep 2014; 8:1365-79; PMID:25159147; http://dx.doi.org/10.1016/j.celrep.2014.07.045

[19] Mateyak MK, Kinzy TG. eEF1A: thinking outside the ribosome. J Biol Chem 2010; 285:21209-13; PMID: 20444696; http://dx.doi.org/10.1074/jbc.R110.113795

[20] Fleischer TC, Weaver CM, McAfee KJ, Jennings JL, Link AJ. Systematic identification and functional screens of uncharacterized proteins associated with eukaryotic ribosomal complexes. Genes Dev 2006; 20:1294-307; PMID:16702403; http://dx.doi.org/10.1101/gad.1422006

[21] Sonenberg N, Hinnebusch AG. Regulation of translation initiation in eukaryotes: mechanisms and biological targets. Cell 2009; 136:731-45; PMID:19239892; http://dx.doi.org/10.1016/j.cell.2009.01.042

[22] Thoreen CC, Chantranupong L, Keys HR, Wang T, Gray NS, Sabatini DM. A unifying model for mTORC1-mediated regulation of mRNA translation. Nature 2012; 485:109-13; PMID:22552098; http://dx.doi.org/10.1038/nature11083

[23] Blobel G, Sabatini D. Dissociation of mammalian polyribosomes into subunits by puromycin. Proc Natl Acad Sci U S A 1971; 68:390-4; PMID:5277091; http://dx.doi.org/10.1073/pnas.68.2.390

[24] Fresno M, Jimenez A, Vazquez D. Inhibition of translation in eukaryotic systems by harringtonine. Eur J Biochem 1977; 72:323-30; PMID:319998; http://dx.doi.org/10.1111/j.1432-1033.1977.tb11256.x

[25] Ingolia NT, Lareau LF, Weissman JS. Ribosome profiling of mouse embryonic stem cells reveals the complexity and dynamics of mammalian proteomes. Cell 2011; 147:789-802; PMID:22056041; http://dx.doi.org/10.1016/j.cell.2011.10.002

[26] Schneider-Poetsch T, Ju J, Eyler DE, Dang Y, Bhat S, Merrick WC, Green R, Shen B, Liu JO. Inhibition of eukaryotic translation elongation by cycloheximide and lactimidomycin. Nat Chem Biol 2010; 6:209-17; PMID: 20118940; http://dx.doi.org/10.1038/nchembio.304

[27] Lee S, Liu B, Huang SX, Shen B, Qian SB. Global mapping of translation initiation sites in mammalian cells at single-nucleotide resolution. Proc Natl Acad Sci U S A 2012; 109:E2424-32; PMID:22927429; http://dx.doi.org/10.1073/pnas.1207846109

[28] Ingolia NT. Ribosome profiling: new views of translation, from single codons to genome scale. Nat Rev Genet 2014; 15:205-13; PMID:24468696; http://dx.doi.org/10.1038/nrg3645

[29] Anger AM, Armache JP, Berninghausen O, Habeck M, Subklewe M, Wilson DN, Beckmann R. Structures of the human and Drosophila 80S ribosome. Nature 2013; 497:80-5; PMID:23636399; http://dx.doi.org/10.1038/nature12104

[30] Arlinghaus R, Shaefer J, Schweet R. Mechanism of Peptide Bond Formation in Polypeptide Synthesis. Proc Natl Acad Sci U S A 1964; 51:1291-9; PMID:14215654; http://dx.doi.org/10.1073/pnas.51.6.1291

[31] Kozak M. Pushing the limits of the scanning mechanism for initiation of translation. Gene 2002; 299:1-34; PMID:12459250; http://dx.doi.org/10.1016/S0378-1119(02)01056-9

[32] Petrov A, Kornberg G, O'Leary S, Tsai A, Uemura S, Puglisi JD. Dynamics of the translational machinery. Curr Opin Struct Biol 2011; 21:137-45; PMID:21256733; http://dx.doi.org/10.1016/j.sbi.2010.11.007

[33] Plotkin JB, Kudla G. Synonymous but not the same: the causes and consequences of codon bias. Nat Rev Genet 2011; 12:32-42; PMID:21102527; http://dx.doi.org/10.1038/nrg2899

[34] Fredrick K, Ibba M. How the sequence of a gene can tune its translation. Cell 2010; 141:227-9; PMID:20403320; http://dx.doi.org/10.1016/j.cell.2010.03.033

[35] Ingolia NT. Genome-wide translational profiling by ribosome footprinting. Methods Enzymol 2010; 470:119-42; PMID:20946809; http://dx.doi.org/10.1016/S0076-6879(10)70006-9

[36] Marguerat S, Schmidt A, Codlin S, Chen W, Aebersold R, Bahler J. Quantitative analysis of fission yeast transcriptomes and proteomes in proliferating and quiescent cells. Cell 2012; 151:671-83; PMID:23101633; http://dx.doi.org/10.1016/j.cell.2012.09.019

[37] Arribere JA, Doudna JA, Gilbert WV. Reconsidering movement of eukaryotic mRNAs between polysomes and P bodies. Mol Cell 2011; 44:745-58; PMID:22152478; http://dx.doi.org/10.1016/j.molcel.2011.09.019

[38] Moore PB. How should we think about the ribosome? Annu Rev Biophys 2012; 41:1-19; PMID:22577819; http://dx.doi.org/10.1146/annurev-biophys-050511-102314

[39] Tourigny DS, Fernandez IS, Kelley AC, Ramakrishnan V. Elongation factor G bound to the ribosome in an intermediate state of translocation. Science 2013; 340:1235490; PMID:23812720; http://dx.doi.org/10.1126/science.1235490

[40] Pulk A, Cate JH. Control of ribosomal subunit rotation by elongation factor G. Science 2013; 340:1235970; PMID:23812721; http://dx.doi.org/10.1126/science.1235970

[41] Zhou J, Lancaster L, Donohue JP, Noller HF. Crystal structures of EF-G-ribosome complexes trapped in intermediate states of translocation. Science 2013; 340:1236086; PMID:23812722; http://dx.doi.org/10.1126/science.1236086

[42] Nolan RD, Grasmuk H, Drews J. The binding of tritiated elongation factors 1 and 2 to ribosomes from Krebs II mouse ascites tumor cells. Eur J Biochem 1975; 50:391-402; PMID:1126342; http://dx.doi.org/10.1111/j.1432-1033.1975.tb09815.x

[43] Mizumoto K, Iwasaki K, Tanaka M, Kaziro Y. Studies on polypeptide elongation factor 2 from pig liver. I. Purification and properties. J Biochem 1974; 75:1047-56; PMID:4607115

[44] Smith KE, Hirsch CA, Henshaw EC. Role of elongation factors and the effect of aurintricarboxylic acid on the synthesis of polyphenylalanine. J Biol Chem 1973; 248:122-30; PMID:4692826

[45] Aspden JL, Eyre-Walker YC, Phillips RJ, Amin U, Mumtaz MA, Brocard M, Couso JP. Extensive translation of small Open Reading Frames revealed by Poly-Ribo-Seq. Elife 2014; 3:e03528; PMID:25144939; http://dx.doi.org/10.7554/eLife.03528

[46] Ruiz-Orera J, Messeguer X, Subirana JA, Alba MM. Long non-coding RNAs as a source of new peptides. Elife 2014; 3:e03523; PMID:25233276; http://dx.doi.org/10.7554/eLife.03523

[47] Fritsch C, Herrmann A, Nothnagel M, Szafranski K, Huse K, Schumann F, Schreiber S, Platzer M, Krawczak M, Hampe J, et al. Genome-wide search for novel human uORFs and N-terminal protein extensions using ribosomal footprinting. Genome Res 2012; 22:2208-18; PMID:22879431; http://dx.doi.org/10.1101/gr.139568.112

[48] Stern-Ginossar N, Weisburd B, Michalski A, Le VT, Hein MY, Huang SX, Ma M, Shen B, Qian SB, Hengel H, et al. Decoding human cytomegalovirus. Science 2012; 338:1088-93; PMID:23180859; http://dx.doi.org/10.1126/science.1227919